Title

Chronic hindbrain administration of oxytocin is sufficient to elicit weight loss in diet-induced obese rats.

Journal

American journal of physiology. Regulatory, integrative and comparative physiology, 313(4)

ISSN

0363-6119

Authors

Roberts, Zachary S
Wolden-Hanson, Tami
Matsen, Miles E
et al.

Publication Date

2017-10-01

DOI

10.1152/ajpregu.00169.2017

Peer reviewed

Am J Physiol Regul Integr Comp Physiol 313: R357–R371, 2017.
First published July 20, 2017; doi:10.1152/ajpregu.00169.2017.

RESEARCH ARTICLE | *Obesity, Diabetes and Energy Homeostasis*

Chronic hindbrain administration of oxytocin is sufficient to elicit weight loss in diet-induced obese rats

Zachary S. Roberts,[1] Tami Wolden-Hanson,[1] Miles E. Matsen,[3] Vitaly Ryu,[5,6] Cheryl H. Vaughan,[5,6] James L. Graham,[4] Peter J. Havel,[4] Daniel W. Chukri,[1] Michael W. Schwartz,[2,3] Gregory J. Morton,[2,3] and James E. Blevins[1,2]

[1]*Veterans Affairs Puget Sound Health Care System, Office of Research and Development, Medical Research Service, Department of Veterans Affairs Medical Center, Seattle, Washington;* [2]*Division of Metabolism, Endocrinology, and Nutrition, Department of Medicine, University of Washington School of Medicine, Seattle, Washington;* [3]*University of Washington Diabetes Institute, University of Washington School of Medicine, Seattle, Washington;* [4]*Departments of Nutrition and Molecular Biosciences, School of Veterinary Medicine, University of California, Davis, California;* [5]*Department of Biology, Georgia State University, Atlanta, Georgia; and* [6]*Center for Obesity Reversal, Georgia State University, Atlanta, Georgia*

Submitted 3 May 2017; accepted in final form 2 July 2017

Roberts ZS, Wolden-Hanson T, Matsen ME, Ryu V, Vaughan CH, Graham JL, Havel PJ, Chukri DW, Schwartz MW, Morton GJ, Blevins JE. Chronic hindbrain administration of oxytocin is sufficient to elicit weight loss in diet-induced obese rats. *Am J Physiol Regul Integr Comp Physiol* 313: R357–R371, 2017. First published July 20, 2017; doi:10.1152/ajpregu.00169.2017.—Oxytocin (OT) administration elicits weight loss in diet-induced obese (DIO) rodents, nonhuman primates, and humans by reducing energy intake and increasing energy expenditure. Although the neurocircuitry underlying these effects remains uncertain, OT neurons in the paraventricular nucleus are positioned to control both energy intake and sympathetic nervous system outflow to interscapular brown adipose tissue (BAT) through projections to the hindbrain nucleus of the solitary tract and spinal cord. The current work was undertaken to examine whether central OT increases BAT thermogenesis, whether this effect involves hindbrain OT receptors (OTRs), and whether such effects are associated with sustained weight loss following chronic administration. To assess OT-elicited changes in BAT thermogenesis, we measured the effects of intracerebroventricular administration of OT on interscapular BAT temperature in rats and mice. Because fourth ventricular (4V) infusion targets hindbrain OTRs, whereas third ventricular (3V) administration targets both forebrain and hindbrain OTRs, we compared responses to OT following chronic 3V infusion in DIO rats and mice and chronic 4V infusion in DIO rats. We report that chronic 4V infusion of OT into two distinct rat models recapitulates the effects of 3V OT to ameliorate DIO by reducing fat mass. While reduced food intake contributes to this effect, our finding that 4V OT also increases BAT thermogenesis suggests that increased energy expenditure may contribute as well. Collectively, these findings support the hypothesis that, in DIO rats, OT action in the hindbrain evokes sustained weight loss by reducing energy intake and increasing BAT thermogenesis.

obesity; brown adipose tissue; thermogenesis; oxytocin

GROWING EVIDENCE SUGGESTS that central release of the neurohypophyseal hormone oxytocin (OT), which is produced predominantly by neurons in the hypothalamic supraoptic nucleus (SON) and paraventricular nucleus (PVN), plays an important role in energy homeostasis (3). Thus, either central or systemic OT can reduce body weight (or body weight gain) in diet-induced obese (DIO) and genetically obese rodent models (1, 7, 17, 33, 35, 40, 45). The translational relevance of these observations was recently buttressed by their successful translation to DIO nonhuman primates (4) and obese humans (32, 56, 61).

The dose-dependent reduction of food intake by OT, whether administered systemically, intranasally, or directly into the central nervous system (CNS), is well documented (3), and while this effect undoubtedly contributes to OT-induced weight loss (4, 7, 17, 33, 59), mounting evidence implies a role for increased energy expenditure (EE) as well. Weight loss elicited by OT exceeds that of pair-fed controls (17, 40). Furthermore, acute third ventricular (3V) or subcutaneous administration of OT increases EE in mice (59, 60) and nonhuman primates (4). Similarly, acute chemogenetic stimulation of PVN OT neurons with use of designer receptors exclusively activated by designer drugs (DREADDs) technology increases both EE and interscapular brown adipose tissue (IBAT) temperature (T_{IBAT}, a functional readout of BAT thermogenesis) in *Oxytocin-Ires-Cre* mice (53a). Conversely, reduced OT signaling is associated with obesity (11, 54, 58, 60), despite the absence of hyperphagia (11, 54), suggesting that EE must also be reduced in this setting (29, 58–60). Indeed, defects in BAT thermogenesis are reported in such models (29, 30). Collectively, these findings support a role for increased BAT thermogenesis in OT-elicited weight loss.

The OT receptor (OTR) populations that mediate the effects of exogenous OT on energy intake and EE remain uncertain. Much work in this field has focused on 3V administration of OT, which reduces high-fat diet (HFD) intake (7, 59, 60), increases EE (59, 60), and evokes weight loss (7, 59, 60), but this route of administration targets OTRs in forebrain and hindbrain and, hence, cannot distinguish between the two regions. In contrast, infusion into the fourth ventricle (4V) targets hindbrain OTRs. Therefore, we sought to determine

Address for reprint requests and other correspondence: J. E. Blevins, VA Puget Sound Health Care System, Research-151, 1660 South Columbian Way, Seattle, WA 98108 (e-mail: jeblevin@u.washington.edu).

whether chronic hindbrain (4V) OT recapitulates the ability of 3V OT to elicit sustained weight loss in rodent models of DIO. We also measured T_{IBAT} during central OT administration to investigate whether OT-elicited weight loss is associated with increased BAT thermogenesis and, if so, whether this effect involves activation of hindbrain OTRs.

Our findings demonstrate that, in a rat model of DIO, chronic hindbrain (4V) administration of OT recapitulates the effects of 3V infusions to reduce both HFD consumption and body fat mass while also elevating T_{IBAT}. We also confirm that OT-mediated stimulation of IBAT thermogenesis involves an OTR-dependent mechanism by showing that the effect is blocked by pretreatment with an OTR antagonist. Collectively, these findings support the hypothesis that sustained weight loss elicited by OT action in the hindbrain in DIO rats likely involves a combination of reduced energy intake and increased BAT thermogenesis.

METHODS

Animals

Adult male Sprague-Dawley (CD IGS) rats (~6.6–7.5 mo old, 477–885 g body wt) and Long-Evans rats (~3–9.25 mo old, 331–781 g body wt) were obtained from Charles River Laboratories International (Wilmington, MA) or Envigo (Indianapolis, IN). C57BL/6J mice (~5.25–6.5 mo old, 25.7–51.3 g body wt) were obtained from The Jackson Laboratory (Bar Harbor, ME). CD IGS rats were used to determine the effect of chronic 4V infusion of OT relative to that of 3V infusion, as previously described (7). The Long-Evans rat strain was chosen by design, given that it is a well-characterized rat model of DIO (55). To determine if these effects occurred across species, additional studies were conducted in C57BL/6J mice. All animals were housed individually in Plexiglas cages in a temperature-controlled (22 ± 2°C) room under a 12:12-h light-dark cycle (lights off at 1 PM). Rats and mice had ad libitum access to water and either a HFD containing 60% of kilocalories from fat (diet no. D12492, Research Diets, New Brunswick, NJ) or a low-fat chow diet containing 13% (rats; diet no. 5001, LabDiet, St. Louis, MO) or 16% (mice; diet no. 5LG4, LabDiet) of kilocalories from fat, unless otherwise stated. Kaolin pellets were also purchased from Research Diets. The research protocols were approved by the Institutional Animal Care and Use Committee of the Veterans Affairs Puget Sound Health Care System (VAPSHCS) and the University of Washington in accordance with National Institutes of Health guidelines for the care and use of animals.

Drug Preparation

Fresh solutions of OT acetate salt (Bachem Americas, Torrance, CA) or the OTR antagonist ($d(CH_2)_5^1$,$Tyr(Me)^2$,Orn^8)-oxytocin trifluoroacetate salt (Bachem Americas) were prepared on the day of each experiment. OT and the OTR antagonist were solubilized in sterile water; OT was further diluted with sterile saline.

3V or 4V Cannulations for Acute Injections

Animals were implanted with a cannula that was directed toward the 3V or 4V, as previously described (6, 7, 39). Briefly, rats or mice under isoflurane anesthesia were placed in a stereotaxic apparatus, with the incisor bar positioned below (3.3 mm for rats or 4.5 mm for mice) the interaural line. A 26-gauge cannula (Plastics One) was stereotaxically positioned into the 3V (rat: 7.3 anterior to the interaural line, 0 mm lateral to the midline, and 7.6 mm ventral to the skull surface; mouse: 1.5 posterior to bregma, 0 mm lateral to the midline, and 4 mm ventral to the skull surface) or 4V (rat: 3.5 posterior to bregma, 1.4 mm lateral to the midline, and 6.2 mm ventral to the skull surface) and secured to the surface of the skull with dental cement and stainless steel screws.

3V or 4V Cannulations for Chronic Infusions

Rats. Briefly, rats were implanted with a cannula within the 3V or 4V with a side port that was connected to an osmotic minipump (model 2004, DURECT, Cupertino, CA), as previously described (7). For rats, we followed the protocol for acute injections described above, except 28-gauge cannulas were placed 1 mm further ventral to the skull surface. The 3V coordinate for the CD IGS rat was also adjusted to 8.1 anterior to the interaural line. A 2.4-inch piece of plastic tubing (Tygon microbore tubing, 0.020 × 0.060 inch OD; Cole-Parmer, Vernon Hills, IL) was tunneled subcutaneously along the midline of the back and connected to the 21-gauge sidearm osmotic minipump-cannula assembly. A stainless steel 22-gauge pin plug (Instech Laboratories, Plymouth Meeting, PA) was inserted at the end of the tubing (backfilled with sterile saline) during a 2-wk postoperative recovery period, after which it was replaced by an osmotic minipump (DURECT) containing saline or OT. Rats were treated with the analgesic buprenorphine SR LAB [sustained release (0.65–1 mg/kg); ZooPharm, Windsor, CO] and the antibiotic enrofloxacin (5 mg/kg; Baytril, Patterson Veterinary, Devens, MA) at the completion of the 3V and 4V cannulations and allowed to recover for ≥10 days before implantation of osmotic minipumps.

Mice. Briefly, mice were implanted with a cannula within the 3V with a side port that was connected to an osmotic minipump (model 2004, DURECT), as previously described (18). Mice under isoflurane anesthesia were placed in a stereotaxic apparatus, with the incisor bar positioned 4.5 mm below the interaural line. A 30-gauge cannula (Plastics One) was stereotaxically positioned into the 3V (1.5 mm caudal to bregma, 0 mm lateral to the midline, and 5 mm ventral to the skull surface) and secured to the surface of the skull with dental cement and stainless steel screws. A 1.2-inch piece of plastic Tygon microbore tubing (0.020 × 0.060 inch OD; Cole-Parmer) was tunneled subcutaneously along the midline of the back and connected to the 21-gauge sidearm osmotic minipump-cannula assembly. A stainless steel 22-gauge pin plug (Instech Laboratories) was inserted at the end of the tubing during a 2-wk postoperative recovery period, after which it was replaced by an osmotic minipump (DURECT) containing saline or OT. Mice were treated with the analgesic ketoprofen (5 mg/kg; Fort Dodge Animal Health) and the antibiotic Baytril (5 mg/kg; Patterson Veterinary) at the completion of the 3V cannulations and allowed to recover for ≥10 days before implantation of osmotic minipumps.

Implantation of Temperature Transponders Beneath IBAT

Animals were anesthetized with isoflurane, the dorsal surface along the upper midline of the back was shaved, and the area was scrubbed with betadine followed by 70% ethanol. A 1-inch incision was made at the midline of the interscapular area. The temperature transponder (14 mm long × 2 mm wide; model HTEC IPTT-300, Bio Medic Data Systems, Seaford, DE) was implanted under one (rat) or both (mouse) IBAT pads, as previously described (9, 57), and secured in place by sterile silk suture. The interscapular incision was closed with standard metal wound clips, which were removed in awake animals 10–14 days after surgery.

Acute 3V or 4V Injections and Measurements of T_{IBAT} in Rats and Mice

OT (or saline vehicle, 1-μl injection volume) was administered immediately before the start of the dark cycle following 6 h of food deprivation in rats or mice. Animals remained without access to food for an additional 4 h during the course of the T_{IBAT} measurements. A hand-held reader (DAS-7007R round implantable programmable temperature transponder wireless reader system, Bio Medic Data Sys-

tems) was used to collect measurements of T_{IBAT} in rats and mice. The 3V and 4V injections were administered at 1 μl/min via an injection pump (model 100 syringe pump, CMA Microdialysis) with a 33-gauge injector (Plastics One) connected by polyethylene-20 tubing to a 10-μl Hamilton syringe. Animals underwent all treatment conditions (unless otherwise noted) in a randomized order, with ≥48 h between treatments. Dose-response studies were conducted to determine a subthreshold dose of the OTR antagonist to use for the experiment.

Body Composition

Lean body mass and fat mass of unanesthetized rats and mice were determined by quantitative magnetic resonance (EchoMRI-700 4-in-1, Echo Medical Systems, Houston, TX) at the VAPSHCS Rodent Metabolic and Behavioral Phenotyping Core.

Study Protocols

Study 1A: effects of chronic 3V OT infusions on energy intake, body weight, and body composition in DIO and chow-fed Long-Evans rats. Ad libitum-fed rats were maintained on chow or the HFD for 4 and 4.5 mo before implantation of 3V cannulas and 28-day minipumps to infuse vehicle or OT (16 nmol/day) over 27 or 28 days. Daily energy intake and body weight were recorded on *days 1–27*.

Study 1B: effects of 3V treatment cessation on energy intake, body weight gain, and body composition in DIO Long-Evans rats. After completion of *study 1A* on *day 27* or *28*, minipumps were removed from a subset of DIO animals under isoflurane anesthesia. Daily energy intake and body weight were recorded in 3-h fasted animals for an additional 27 days.

Study 2A: effects of chronic 3V OT infusions on energy intake, body weight, and body composition in DIO and chow-fed mice. Ad libitum-fed mice were maintained on chow or the HFD for 4 and 4.5 mo before implantation of 3V cannulas and 28-day minipumps for infusion of vehicle or OT (16 nmol/day) over 28 days, respectively. Daily energy intake and body weight were recorded on *days 1–28*.

Study 2B: effect of chronic 3V OT infusions on kaolin consumption in DIO mice. Kaolin intake (g) was assessed across 15 days following implantation of minipumps containing vehicle (saline) or OT (16 nmol/day). Placement of kaolin and chow was reversed every other day within each treatment condition.

Study 3A: effects of chronic 4V OT infusions on energy intake, body weight, and body composition in DIO and chow-fed CD IGS rats. Ad libitum-fed rats were maintained on chow or the HFD for 4 and 4.5 mo before implantation of 4V cannulas and 28-day minipumps for infusion of vehicle or OT (16 nmol/day) over 27 days, respectively. Daily energy intake and body weight were recorded on *days 1–27*.

Study 3B: effect of chronic 4V OT infusions on kaolin consumption in DIO CD IGS rats. Kaolin intake (g) was assessed across 27 days following implantation of minipumps containing vehicle (saline) or OT (16 nmol/day). Placement of kaolin and chow was reversed every other day within each treatment condition.

Study 3C: effects of 4V treatment cessation on energy intake, body weight gain, and body composition in DIO CD IGS rats. After completion of *study 3A* on *day 27*, minipumps were removed from a subset of DIO animals under isoflurane anesthesia. Daily energy intake and body weight were recorded in 3-h-fasted animals for an additional 27 days.

Study 4A: effects of chronic 4V OT infusions on energy intake, body weight, and body composition in DIO Long-Evans rats. Ad libitum-fed rats were maintained on chow or the HFD for 4 and 4.5 mo before implantation of 4V cannulas and 28-day minipumps for infusion of vehicle or OT (16 nmol/day) over 27 days, respectively. Daily energy intake and body weight were recorded on *days 1–27*.

Study 4B: effects of 4V treatment cessation on energy intake, body weight gain, and body composition in DIO Long-Evans rats. After completion of *study 4A* on *day 27*, minipumps were removed from a subset of DIO animals under isoflurane anesthesia. Daily energy intake and body weight were recorded in 3-h-fasted animals for an additional 27 days.

Study 5: effects of acute 3V OT administration on T_{IBAT} in rats and mice. 3V cannulas and temperature transponders were implanted in rats and mice. After adaptation to a 6-h fast and handling, vehicle or OT [1 and 5 μg/μl (rats), 5 μg/μl (mice)] was injected into the 3V immediately before the start of the dark cycle in a crossover design at 48-h intervals, such that each animal served as its own control. T_{IBAT} was measured at baseline (−2 h), immediately before 3V injections (0 h), and at 0.25, 0.5, 0.75, 1, 1.25, 1.5, 2, 3, 4, and 18 h postinjection.

Study 6A: effects of acute 4V OT administration on T_{IBAT} in rats. 4V cannulas and temperature transponders were implanted in rats. After adaptation to a 6-h fast and handling, vehicle or OT (1 and 5 μg/μl) was injected into the 4V immediately before the start of the dark cycle in a crossover design at 48-h intervals, such that each animal served as its own control. T_{IBAT} was measured at baseline (−2 h), immediately before 4V injections (0 h), and at 0.25, 0.5, 0.75, 1, 1.25, 1.5, 2, 3, 4, and 18 h postinjection.

Study 6B: effects of 4V OT administration on T_{IBAT} following 4V OT antagonist treatment in rats. 4V cannulas and temperature transponders were implanted in rats. After adaptation to a 6-h fast and handling, vehicle (2 μl) or the OT receptor antagonist (10 μg in 2 μl) was injected into the 4V 30 min before OT (5 μg/μl) in a crossover design at 48-h intervals, such that each animal served as its own control. As described above, T_{IBAT} was measured at baseline (−2 h), immediately before 4V injections (0 h), and at 0.25, 0.5, 0.75, 1, 1.25, 1.5, 2, 3, 4, and 18 h postinjection.

Study 6C: effects of acute 4V OT administration on T_{IBAT} in DIO rats. 4V cannulas and temperature transponders were implanted in rats. After adaptation to a 6-h fast and handling, vehicle or OT (1 and 5 μg/μl) was injected into the 4V immediately before the start of the dark cycle in a crossover design at 48-h intervals, such that each animal served as its own control. T_{IBAT} was measured at baseline (−2 h), immediately before 4V injections (0 h), and at 0.25, 0.5, 0.75, 1, 1.25, 1.5, 2, 3, 4, and 18 h postinjection.

Study 6D: effects of chronic 3V OT administration on T_{IBAT} in DIO rats. 3V cannulas and temperature transponders were implanted in a subset of rats from *study 1A*. T_{IBAT} was measured once daily over the first 3 days of the infusion period in 3-h-fasted rats.

Blood Collection

Blood was collected from 3-h-fasted rats and mice at the end of the light cycle within a 2-h window (10:00 AM–12:00 PM), as previously described in DIO CD IGS rats (7). Treatment groups were counterbalanced at euthanasia to avoid bias. Blood samples [up to 3 ml (rats) or 0.5 ml (mice)] were collected immediately before transcardial perfusion by cardiac puncture in chilled serum separator tubes (Amber SST, Becton Dickinson, Franklin Lakes, NJ). Whole blood was centrifuged at 6,000 rpm for 1.5 min at 4°C; serum was removed, separated into aliquots, and stored at −80°C for analysis.

Serum Hormone Measurements

Serum leptin was measured using electrochemiluminescence detection [Meso Scale Discovery (MSD), Rockville, MD] using established procedures (8). Intra-assay coefficient of variation (CV) for leptin was 3.9%. The range of detectability for the leptin assay is 0.055–100 ng/ml. Serum fibroblast growth factor-21 (FGF-21; R & D Systems, Minneapolis, MN) and irisin (AdipoGen, San Diego, CA) levels were determined by ELISA. The intra-assay CVs for FGF-21 and irisin were 4.3 and 4.1%, respectively; the ranges of detectability were 13.4–2,000 pg/ml for FGF-21 and 0.1–5 μg/ml for irisin. Data were normalized to historical values using a pooled plasma quality-control sample that was assayed in each plate.

Blood Glucose and Lipid Measurements

Blood was collected for glucose measurements by tail vein nick and measured using a glucometer and a blood glucose monitoring system (AlphaTRAK 2, Abbott Laboratories, Abbott Park, IL) (7). Total cholesterol (TC) and free fatty acids (FFAs) were measured using an enzymatic-based kit (Wako Chemicals USA, Richmond, VA). Intra-assay CVs for TC and FFAs were 1.2 and 1.1%, respectively. These assay procedures have been validated for rodents (16).

Statistical Analyses

Values are means ± SE. Comparisons between multiple groups involving between-subjects designs were made using one- or two-way ANOVA as appropriate, followed by a post hoc Fisher's least significant difference test. Comparisons involving within-subjects designs were made using a one-way repeated-measures ANOVA followed by a post hoc Fisher's least significant difference test. Analyses were performed using the statistical program SYSTAT (Systat Software, Point Richmond, CA). Differences were considered significant at $P < 0.05$ (2-tailed).

RESULTS

Study 1A: Effects of Chronic 3V OT Infusions on Energy Intake, Body Weight, and Body Composition in DIO and Chow-Fed Long-Evans Rats

Our previous work demonstrates that chronic 3V OT administration is sufficient to prevent and reverse DIO in CD IGS rats (7). To determine if this effect is consistent across other DIO rat models, we studied Long-Evans rats, which exhibit increased susceptibility to DIO (55) and are widely used in the literature. As expected, Long-Evans rats fed the HFD for 4.5 mo gained more weight (600 ± 12 vs. 519 ± 13 g) and exhibited greater adiposity (192 ± 9 vs. 92 ± 9 g) than chow-fed controls ($P < 0.05$) before 3V administration of OT or vehicle.

Whereas rats maintained on the HFD and treated with 3V vehicle continued to gain weight throughout the 28-day study period, rats maintained on the HFD and treated with 3V OT exhibited marked reductions of total body weight (~6.3%; Fig. 1*A*) and weight gain (Fig. 1*B*) relative to baseline values ($P < 0.05$). This effect was associated with sustained reductions of fat mass gain (Fig. 1*C*; $P < 0.05$) and serum leptin levels (Table 1), with no decrease in lean mass gain. As expected, a sustained reduction of energy intake was associated with these OT-mediated changes in body weight and composition (Fig. 1*D*; $P < 0.05$).

To determine if these effects of OT depend on nutritional status, the above-described studies were repeated in age-matched nonobese chow-fed rats. While body weight gradually increased throughout the 28-day study period in the 3V-vehicle group, but not the 3V-OT group (Fig. 1*E*; $P < 0.05$), 3V OT did not induce weight loss [Fig. 1, *E* and *F*; P = not significant (NS)], as observed in DIO rats. Furthermore, there were no differences in fat mass gain or lean mass gain (Fig. 1*G*; P = NS) or energy intake (Fig. 1*H*; P = NS) between 3V-vehicle and 3V-OT cohorts of chow-fed animals.

At the dose selected for this study (16 nmol/day), therefore, the effect of 3V OT to elicit reduced fat mass and weight loss appears selective for rats with DIO; in these animals, loss of body weight was confined to the adipose tissue compartment, with no overall effect on lean body mass. Whereas a lower dose of 3V OT (1.6 nmol/day) was without effect on weight gain in Long-Evans and CD IGS rats (7) that were maintained on a HFD but did not have established DIO (data not shown), a more complete dose-response analysis is needed to determine if selectivity for DIO holds across effective OT doses.

Study 1B: Effects of 3V Treatment Cessation on Energy Intake, Body Weight Gain, and Body Composition in DIO Long-Evans Rats

We previously showed that the reduction of weight gain following OT treatment persists for ~10 days in CD IGS rats (7). To determine the durability of effects on energy balance and body composition following cessation of OT treatment in Long-Evans rats with DIO, we tracked daily energy intake and body weight following minipump removal in a subset of animals used in *study 1A*. In vehicle-treated animals, body weight remained stable following minipump removal (on *day 27* or *28*), as expected. By comparison, body weight significantly increased in animals that previously received OT (Fig. 2*A*; $P < 0.05$) but remained significantly below that of vehicle-treated controls for the next ~12 days (Fig. 2*B*; $P < 0.05$). Eventually, however, the effect of 3V OT to reduce body weight, fat mass, and serum leptin levels (Table 1) in these animals subsided, with values returning to those of vehicle-treated controls (Fig. 2*C*; P = NS). This response appears to have been driven by a rebound hyperphagia that developed during the 2nd wk following minipump removal (Fig. 2*D*).

Serum Hormones Following 3V Vehicle and OT Treatment and Treatment Cessation in Chow- and HFD-Fed Long-Evans Rats

To characterize the metabolic effects of 3V OT in DIO and chow-fed Long-Evans rats, we measured blood glucose levels and serum concentrations of leptin, insulin, FGF-21, irisin, TC, and FFAs. At baseline, vehicle-treated DIO animals exhibited increased levels of leptin, insulin, FGF-21, irisin, and TC relative to chow-fed vehicle-treated animals ($P < 0.05$; Table 1). As expected, OT treatment was associated with a reduction of serum leptin in DIO animals (7, 17) (in which fat mass was also reduced), but not in chow-fed control animals (in which fat mass was not reduced). As reported earlier (7), 3V OT also reduced serum TC levels ($P < 0.05$) in DIO, but not chow-fed, animals. In contrast, OT treatment was not associated with significant changes in blood glucose levels or serum levels of insulin, FGF-21, irisin, or FFA in DIO or chow-fed rats. After the washout period, differences in serum leptin or TC levels between animals that received OT or vehicle treatment were no longer apparent (P = NS; Table 1).

Study 2, A and B: Effects of Chronic 3V OT Infusions on Energy Intake, Body Weight, and Body Composition in DIO and Chow-Fed Mice

To determine whether the weight-reducing effect of chronic 3V OT infusion in two DIO rat models extends to obese mice, we repeated these studies in age-matched DIO and chow-fed C57BL/6J mice. By design, body weight (43.4 ± 1.1 vs. 30.8 ± 0.6 g) and adiposity (17 ± 0.5 vs. 3.7 ± 0.6 g) were greater ($P < 0.05$) in DIO than chow-fed mice at baseline (after maintenance on chow or the HFD for 4.5 mo).

In contrast to continuous body weight gain during 3V vehicle treatment over 28 days in DIO mice maintained on the HFD (Fig. 3*A*; $P < 0.05$), 3V OT treatment induced reduc-

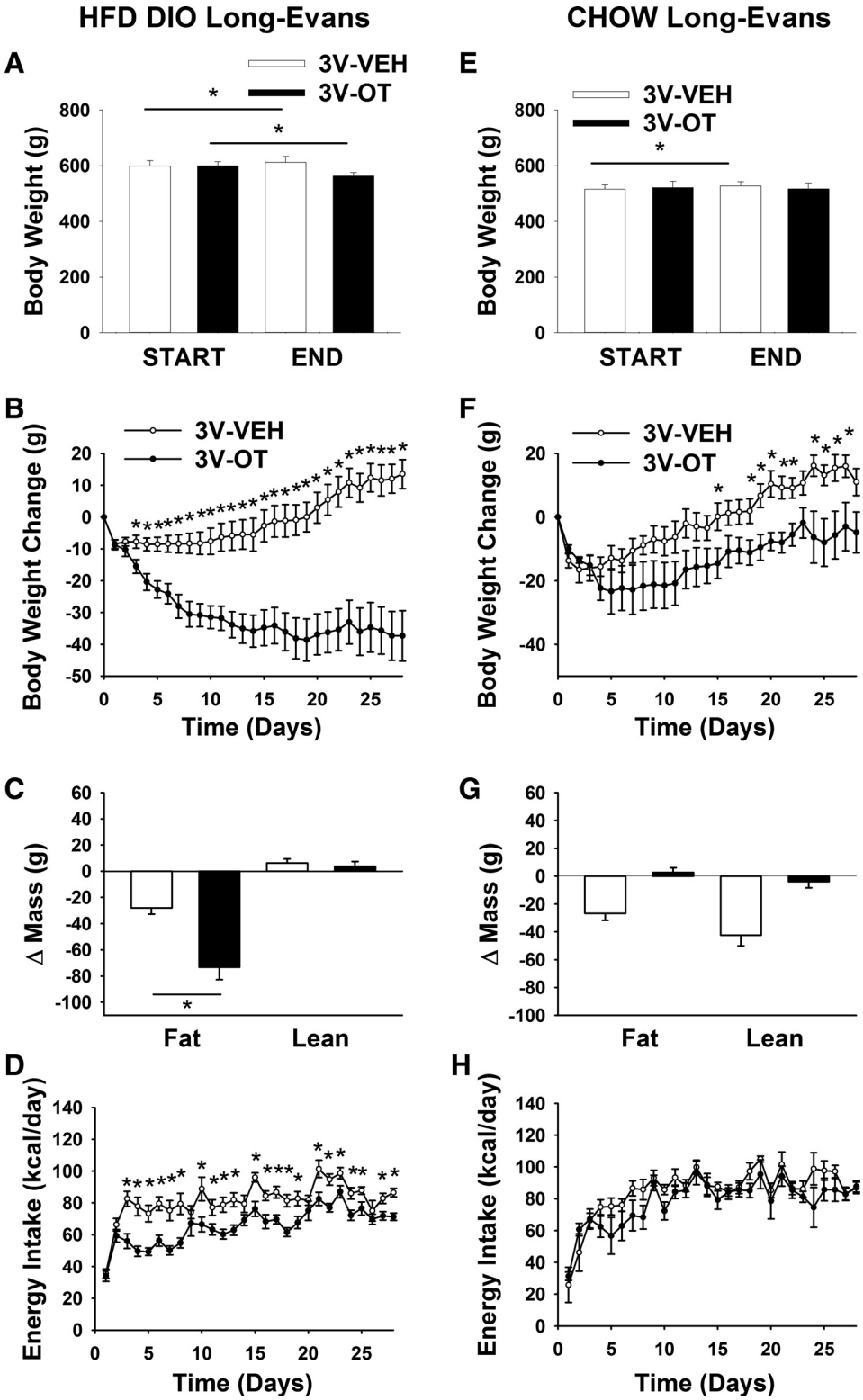

Fig. 1. Effects of chronic oxytocin (OT) infusion into the 3rd ventricle (3V) on energy intake, body weight, and body composition in diet-induced obese (DIO) and chow-fed Long-Evans rats. Ad libitum-fed rats were maintained on the high-fat diet (HFD; 60% of kcal from fat; n = 17–18/group) or chow (n = 6–7/group) for 4.5 mo before receiving continuous infusions of vehicle (Veh) or OT (16 nmol/day). *A* and *E*: change in body weight in HFD-fed DIO and chow-fed control animals. *B* and *F*: change in body weight gain in HFD-fed DIO and chow-fed control animals. *C* and *G*: change in fat mass and lean mass in HFD-fed DIO and chow-fed control animals. *D* and *H*: daily energy intake in HFD-fed DIO and chow-fed control animals. Values are means ± SE. *$P < 0.05$, OT vs. vehicle.

tions of body weight (~8.7%; Fig. 3*A*) and weight gain (Fig. 3*B*) relative to the start of the infusion period ($P < 0.05$). There was a significant main effect of OT to reduce fat mass gain (Fig. 3*C*; $P = 0.05$), with no effect on lean body mass, as in DIO rats, effects that were mediated, at least in part, by a reduction of energy intake over the first 2 wk (Fig. 3*D*; $P < 0.05$). These effects do not appear to result from an aversive effect of 3V OT, since there was no effect on kaolin consumption (relative to vehicle-treated DIO control mice; n = 3–5/group) during the 12-day measurement period (P = NS; data not shown). Overall, these findings demonstrate that the response of DIO mice to 3V OT is similar to that of

Table 1. *Serum measurements after 3V infusions of OT or vehicle and at washout in DIO rats from study 3A*

	Chow		HFD		HFD	
	Veh	OT	Veh	OT	Veh Washout	OT Washout
Leptin, ng/ml	10.4 ± 2.4[c]	7.0 ± 1.6[c]	28.1 ± 1.9[a]	18.7 ± 2.4[b]	28.5 ± 2.3[a]	31.5 ± 2.5[a]
Insulin, ng/ml	0.6 ± 0.09[c]	0.8 ± 0.02[a,c]	1.3 ± 0.20[a,b]	1.3 ± 0.23[b]	4.4 ± 1.30[a]	5.0 ± 1.38[a]
FGF-21, pg/ml	51 ± 4.7[b]	53 ± 14.9[b,c]	97 ± 12.5[a]	73 ± 6.1[a,b]	108 ± 11.4[a]	108 ± 15.1[a]
Irisin, μg/ml	3.5 ± 0.2[b]	5.0 ± 0.3[a,b]	5.7 ± 0.7[a]	5.7 ± 0.5[a]	5.3 ± 0.3[a]	4.4 ± 0.2[a]
Blood glucose, mg/dl	143 ± 5.3[a]	143 ± 4.4[a]	141 ± 3.8[a]	149 ± 5.5[a]	137 ± 4.9[a]	142 ± 5.6[a]
FFA, meq/l	0.2 ± 0.02[b,c]	0.1 ± 0.02[c]	0.3 ± 0.02[a]	0.2 ± 0.06[a,b]	0.3 ± 0.06[a]	0.3 ± 0.03[a]
Total cholesterol, mg/dl	61 ± 3.2[c]	61 ± 3.4[c,d]	85 ± 2.1[a]	72 ± 3.4[b]	75 ± 5.5[a]	81 ± 2.9[a]

Values means ± SE; n = 6–7/group for oxytocin (OT)- or vehicle (Veh)-infused rats; n = 9–11/group for washout rat. 3V, 3rd ventricle; DIO, diet-induced obese; HFD, high-fat diet. Different superscript letters denote significant differences between treatments; shared letters denote values that are not significantly different from one another.

DIO rats and extend previous evidence that neither acute nor chronic 3V administration of OT affects kaolin consumption (7, 59).

Similar to our observations in rats, the weight-reducing effect of 3V OT in HFD-fed DIO mice was not observed in mice fed standard chow (Fig. 3*E*; P = NS), although a slight attenuation of weight gain relative to 3V vehicle-treated controls was observed over the 28-day period (Fig. 3*F*; $P < 0.05$). This modest effect was not associated with significant changes in body fat mass or lean mass (Fig. 3*G*; P = NS) or energy intake (Fig. 3*H*) relative to vehicle-treated controls.

Serum Hormones Following 3V Vehicle and OT Treatment in Chow- and HFD-Fed DIO Mice

Among animals receiving 3V vehicle, mice maintained on the HFD exhibited increased levels of blood glucose and serum leptin, insulin, FGF-21, blood glucose, and TC relative to those fed standard chow ($P < 0.05$; Table 2). Similar to observations in the DIO rat model, 3V OT failed to reduce serum insulin levels but did reduce serum TC levels ($P < 0.05$), whereas blood glucose and serum levels of leptin, FFA, TG, irisin, and FGF-21 were not significantly altered.

Study 3A: Effects of Chronic 4V OT Infusions on Energy Intake, Body Weight, and Body Composition in DIO and Chow-Fed CD IGS Rats

Given that *1*) the 3V route of administration does not differentiate a forebrain from a hindbrain site of action and *2*) intake of standard chow is acutely inhibited by 4V (27, 43) or nucleus tractus solitarius (NTS) administration of OT (43), we sought to determine whether the antiobesity effects of chronic 3V OT administration are replicated by chronic hindbrain (4V) OT administration in either of two different DIO rat (CD IGS and Long-Evans) models.

As expected, body weight (738 ± 13 vs. 614 ± 13 g) and fat mass (226 ± 9 vs. 113 ± 9 g) were greater in CD IGS rats that had been maintained on the HFD for 4.5 mo than in age-matched chow-fed rats ($P < 0.05$) at study onset.

Consistent with the response to 3V OT, continuous 4V OT infusion over 27 days reduced body weight (~4.9%; Fig. 4*A*) and body weight gain (Fig. 4*B*) in HFD-fed CD IGS rats ($P < 0.05$), effects associated with reduced fat mass gain. In contrast to chronic 3V OT administration, however, 4V OT administration also reduced lean mass gain (Fig. 4*C*; $P < 0.05$). These effects were again associated with a sustained reduction of energy intake (Fig. 4*D*; $P < 0.05$) that was not secondary to an aversive effect of 4V OT, since kaolin consumption was not increased (data not shown).

Consistent with results from 3V OT administration, these effects of chronic 4V OT administration appear to be specific for DIO animals, since, despite a small transient effect at study onset, 4V OT did not reduce body weight, fat mass, or energy intake in chow-fed control CD IGS rats at the dose used (16 nmol/day; Fig. 4, *D–G*). Future studies are needed to determine if the diet-selective nature of the response to 4V OT pertains across the effective dose range.

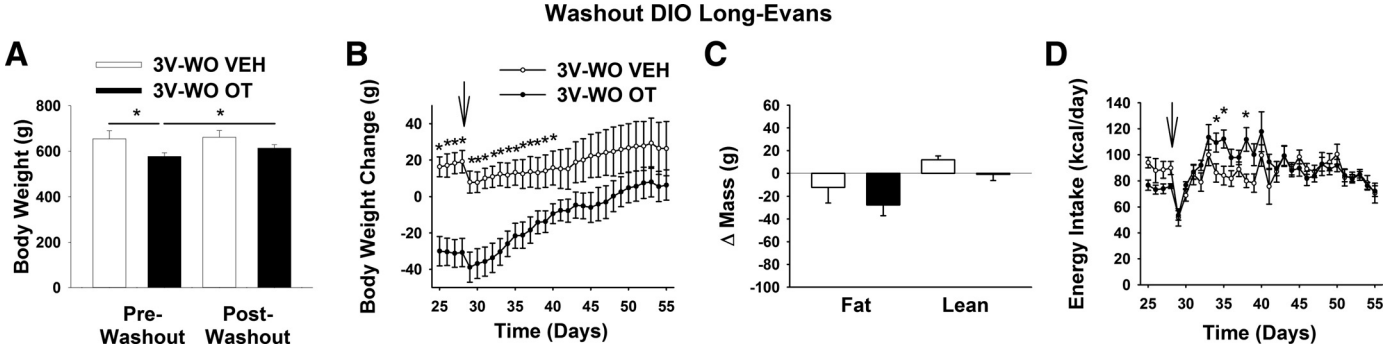

Fig. 2. Effects of 3V OT treatment cessation on energy intake, body weight gain, and body composition in DIO Long-Evans rats. Minipumps were removed on *day 27* (indicated by arrow) from a subset of DIO rats (n = 7–11/group) that previously received continuous infusions of vehicle or OT (16 nmol/day). Ad libitum-fed rats were maintained on the HFD (60% of kcal from fat) throughout the 27-day washout (WO) period. *A*: change in body weight in HFD-fed DIO animals during washout. *B*: change in body weight gain in HFD-fed DIO animals during washout. *C*: change in fat mass and lean mass in HFD-fed DIO animals during washout. *D*: daily energy intake in HFD-fed DIO animals during washout. Values are means ± SE. *$P < 0.05$, OT vs. vehicle or post-OT vs. postvehicle.

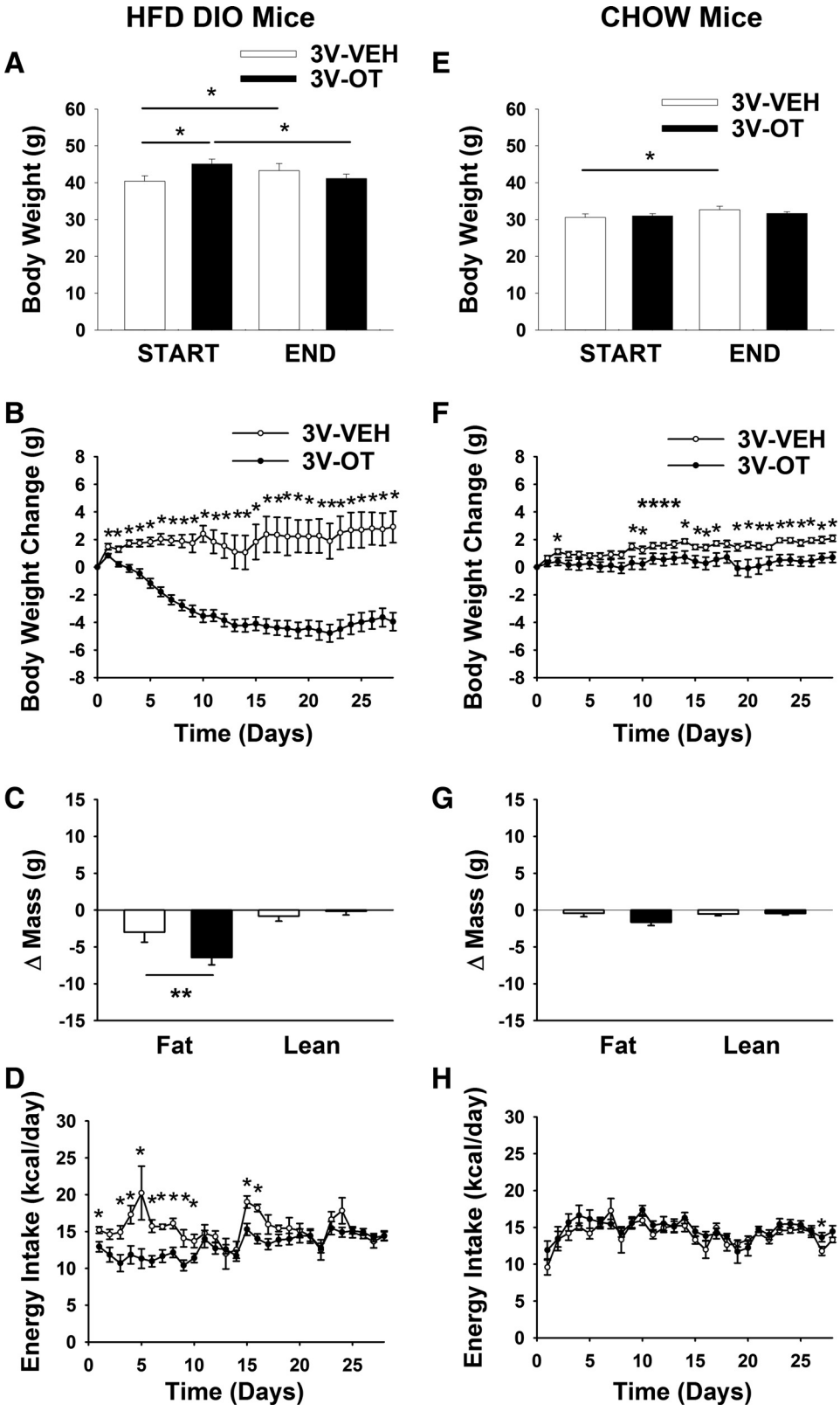

Fig. 3. Effects of chronic 3V OT infusions on energy intake, body weight gain, and body composition in DIO and chow-fed mice. Ad libitum-fed mice were maintained on the HFD (60% of kcal from fat; $n = 7$–12/group) or chow ($n = 8$–9/group) for 4.5 mo before receiving continuous infusions of vehicle or OT (16 nmol/day). *A* and *E*: change in body weight in HFD-fed DIO and chow-fed control animals. *B* and *F*: change in body weight gain in HFD-fed DIO and chow-fed control animals. *C* and *G*: change in fat mass and lean mass in HFD-fed DIO and chow-fed control animals. *D* and *H*: daily energy intake in HFD-fed DIO and chow-fed control animals. Values are means ± SE. $^{*}P < 0.05$, $^{**}P = 0.05$, OT vs. vehicle.

Overall, these data indicate that chronic 4V delivery of OT elicits sustained reductions of energy intake, body weight, weight gain, and fat mass gain in DIO (but not chow-fed) rats. Since 4V OT had no effect on kaolin intake in HFD-fed rats and did not suppress energy intake in chow-fed rats, the substantial weight reduction induced by hindbrain OT action in this DIO rat model does not appear to involve an aversive effect.

Table 2. *Serum measurements following 3V infusions of OT or vehicle in DIO mice from study 7*

	Chow		HFD	
	Veh	OT	Veh	OT
Leptin, ng/ml	1.9 ± 0.6[a]	1.4 ± 0.2[a]	22.9 ± 5.4[b]	14.9 ± 4.0[b]
Insulin, ng/ml	0.2 ± 0.03[a]	0.2 ± 0.02[a]	0.5 ± 0.14[b]	0.5 ± 0.14[b]
FGF-21, pg/ml	138 ± 26[a]	134 ± 14[a]	694 ± 156[b]	652 ± 152[b]
Irisin, μg/ml	2.3 ± 0.2	2.0 ± 0.1	1.9 ± 0.2	2.1 ± 0.2
Blood glucose, mg/dl	197 ± 7.5[a,b]	190 ± 12.0[b]	228 ± 15.9[a]	211 ± 4.7[a,b]
FFA, meq/l	0.3 ± 0.04[a]	0.2 ± 0.01[a,c]	0.2 ± 0.05[c]	0.2 ± 0.02[c]
Total cholesterol, mg/dl	122 ± 6.6[a]	93 ± 6.7[a]	230 ± 17.4[b]	196 ± 22.7[c]

Values means ± SE; n = 3–12/group. Different superscript letters denote significant differences between treatments; shared letters denote values that are not significantly different from one another.

Study 3B: Effects of 4V Treatment Cessation on Energy Intake, Body Weight Gain, and Body Composition in DIO CD IGS Rats

To assess the reversibility of 4V OT-elicited reductions in weight gain, fat mass, and energy intake, these parameters were monitored following cessation of treatment. As observed following 3V OT treatment, animals maintained their weight loss for ~5 days following 4V OT treatment relative to 4V vehicle controls (Fig. 5, *A* and *B*; $P < 0.05$), but differences in body weight and fat mass eventually disappeared (Fig. 5*C*; P = NS). Interestingly, this occurred despite the lack of rebound hyperphagia (Fig. 5*D*; P = NS).

Study 4A: Effects of Chronic 4V OT Infusions on Energy Intake, Body Weight, and Body Composition in DIO Long-Evans Rats

To extend our findings to another rat model of DIO, we examined the effects of chronic hindbrain (4V) OT administration (~27 days) in Long-Evans rats maintained on a HFD (55). After HFD exposure for 4.5 mo, DIO Long-Evans rats weighed 567 ± 10 g and had a total fat mass of 194 ± 10 g at study onset.

Consistent with the effect of 3V OT in this rat model, we found that chronic 4V delivery of OT elicits sustained reductions of body weight (~5.8%; Fig. 6*A*), weight gain (Fig. 6*B*), and fat mass gain (Fig. 6*C*; $P < 0.05$) while preserving lean mass, effects associated with a sustained reduction of energy intake (Fig. 6*D*). These effects closely resemble those elicited by 4V OT in CD IGS rats (Fig. 4).

Study 4B: Effects of 4V Treatment Cessation on Energy Intake, Body Weight Gain, and Body Composition in DIO Long-Evans Rats

After cessation of 4V infusion (minipump removal on *day 27*), body weight increased in both OT- and vehicle-treated groups (Fig. 6*E*; $P < 0.05$), although the weight reduction elicited by 4V OT persisted for ~4 days (Fig. 6*F*; $P < 0.05$) and the associated reduction of fat mass disappeared by the end of the study period (27 days following minipump removal; Fig. 6*G*; P = NS). Recovery of lost weight in 4V OT animals was associated with a transient increase in energy intake that was evident only during the 3rd wk following minipump removal (Fig. 6*H*; $P < 0.05$).

Blood glucose levels following 4V infusion of OT (152.5 ± 4.4) did not differ from 4V vehicle-treated controls (156.3 ± 4; P = NS).

Study 5: Effects of Acute 3V OT Administration on T_{IBAT} in Rats and Mice

Given that *1*) BAT activation plays a key role in control of thermogenesis in rodents (12, 36–38), *2*) reduced energy intake cannot fully explain OT-elicited weight loss (17, 40), and *3*) 3V OT administration increases EE in rodents (59, 60), we hypothesized that the antiobesity effect of OT in the CNS involves increased EE arising from stimulation of BAT thermogenesis.

Consistent with this hypothesis, we found that, in chow-fed Long-Evans rats, T_{IBAT} was increased by 3V OT at 1- and 5-μg doses throughout the 2-h measurement period. Specifically, OT (1 μg) increased T_{IBAT} at 0.5, 0.75, 1 ($P = 0.051$), 1.5, 1.75, and 2 h postinjection (data not shown; $P < 0.05$). Similar effects were observed with the higher (5-μg) dose of 3V OT (Fig. 7*A*; $P < 0.05$).

To determine whether 3V OT increases T_{IBAT} across rodent species, we repeated these studies in chow-fed C57BL/6J mice. As in rats, 3V OT increased T_{IBAT} at the 5-μg dose throughout the measurement period (Fig. 7*B*; $P < 0.05$). Collectively, these observations offer compelling evidence that BAT thermogenesis increases in response to the central action of OT but does not inform the brain area(s) responsible for this effect.

Study 6A: Effects of Acute 4V OT Administration on T_{IBAT} in Rats

To investigate whether hindbrain OTRs contribute to the effects of 3V OT to stimulate BAT thermogenesis, we measured the effect of 4V administration of OT on T_{IBAT} in chow-fed Long-Evans rats. Consistent with this hypothesis, T_{IBAT} increased following 4V administration of OT (1 and 5 μg), and this effect was again sustained throughout the 2-h monitoring period in a manner similar to that observed following 3V OT (Fig. 8*A*; $P < 0.05$).

Study 6B: Effects of 4V OT Administration on T_{IBAT} Following 4V OT Antagonist Treatment in Rats

To confirm that this effect of 4V OT to increase T_{IBAT} is mediated specifically through OTRs, chow-fed Long-Evans rats were treated with a 4V injection of the OTR antagonist d(CH_2)$_5^1$,Tyr(Me)^2,Orn^8]-OT or vehicle before a second 4V injection of OT or vehicle. As expected, the effect of 4V OT to increase T_{IBAT} was fully blocked following administration of a dose of the OTR antagonist that did not alter T_{IBAT} when given alone (Fig. 8*B*).

Two-way ANOVA revealed a significant main effect of 4V OT [$F(1,33) = 8.137$, $P < 0.05$] and 4V OTR antagonist [$F(1,33) = 12.772$, $P < 0.05$] and a significant interactive effect of the 4V OTR antagonist to block the effects of 4V OT on T_{IBAT} [$F(1,33) = 6.709$, $P < 0.05$].

These findings indicate that hindbrain (4V) administration of OT elevates T_{IBAT} through an OTR-dependent mechanism.

Study 6C: Effects of Acute 4V OT Administration on T_{IBAT} in DIO Rats

To test whether DIO impacts the T_{IBAT} response to central OT, the study was repeated in the HFD-fed Long-Evans rat model. We found that 4V administration of OT (5 μg) in-

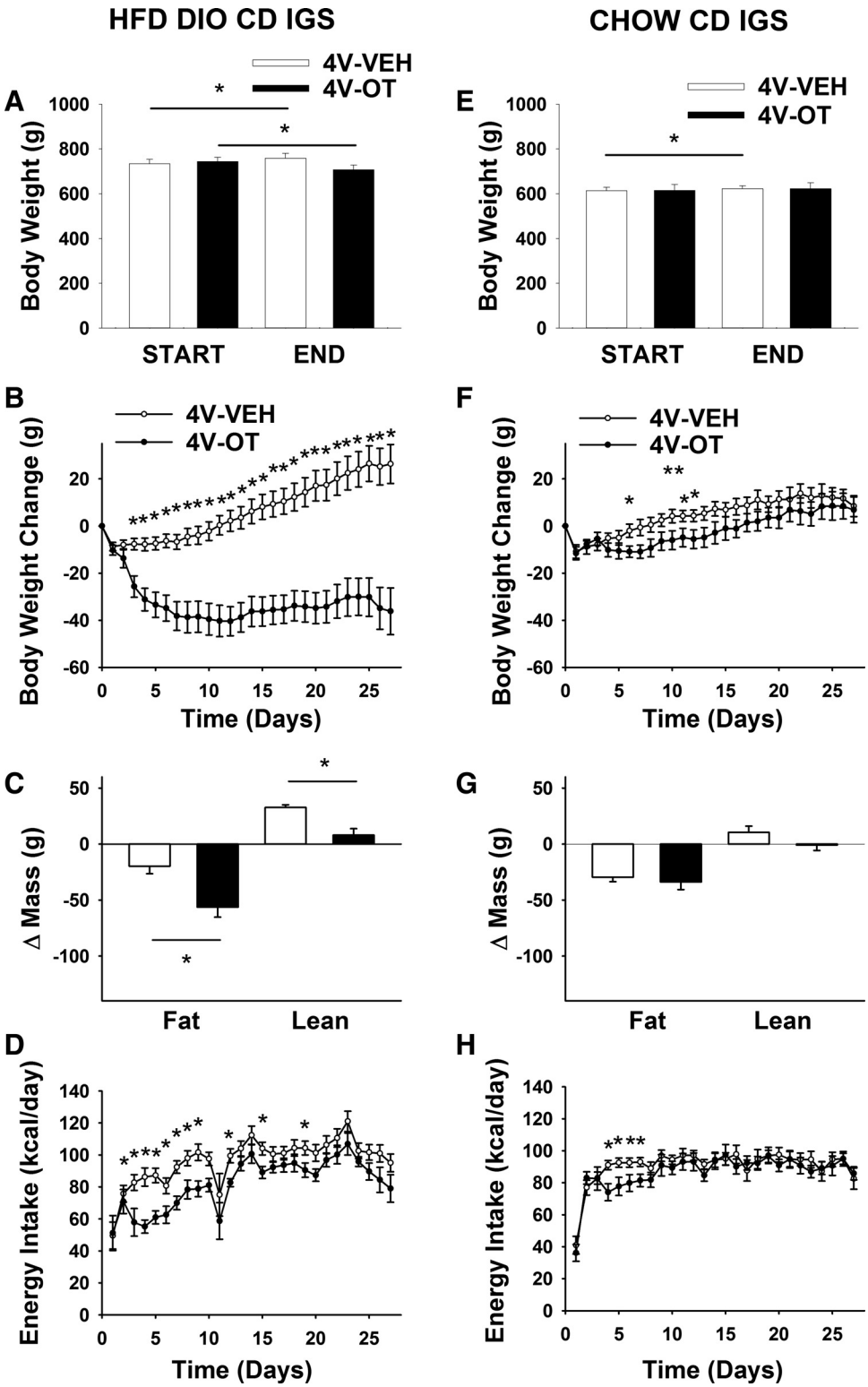

Fig. 4. Effects of chronic 4V OT infusions on energy intake, body weight gain, and body composition in DIO and chow-fed CD IGS rats. Ad libitum-fed rats were maintained on the HFD (60% of kcal from fat; n = 12–15/group) or chow (n = 7–11/group) for 4.5 mo before receiving continuous infusions of vehicle or OT (16 nmol/day). *A* and *E*: change in body weight in HFD-fed DIO and chow-fed control animals. *B* and *F*: change in body weight gain in HFD-fed DIO and chow-fed control animals. *C* and *G*: change in fat mass and lean mass in HFD-fed DIO and chow-fed control animals. *D* and *H*: daily energy intake in HFD-fed DIO and chow-fed control animals. Values are means ± SE. *$P < 0.05$, OT vs. vehicle.

creased T_{IBAT} in a manner largely comparable to that observed in nonobese, chow-fed rats (Fig. 8*C*).

Study 6D: Effects of Chronic 3V OT Administration on T_{IBAT} in DIO Rats

To determine if effects on T_{IBAT} following acute 3V or 4V OT administration are also detected with chronic OT administration, T_{IBAT} was measured during chronic 3V delivery during the initial period of OT-elicited weight loss (over the first 3 days) in the DIO Long-Evans rat model. We found that chronic 3V infusion of OT (16 nmol/day) increased T_{IBAT} during infusion *days 2* and *3*, a period that coincides with the initial weight-lowering effect following chronic 3V administration of OT (Fig. 1*B*). These findings support a role for

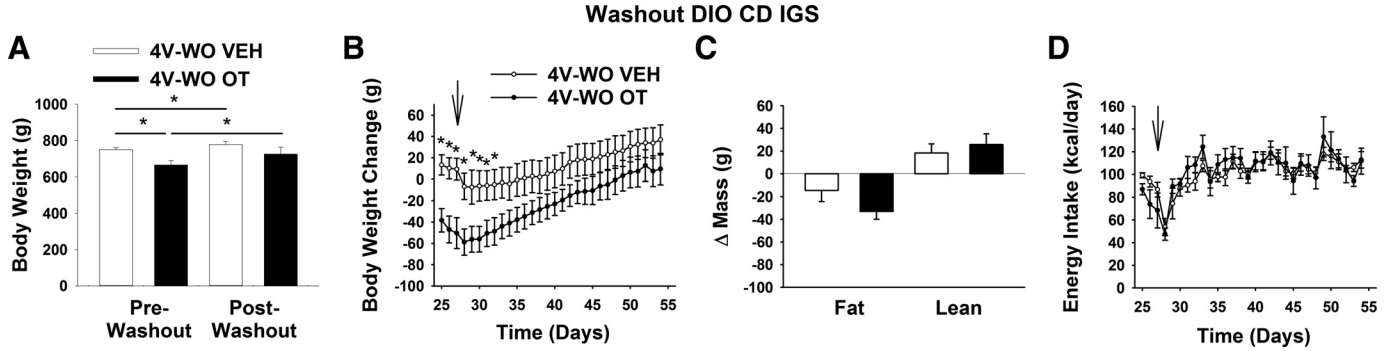

Fig. 5. Effects of 4V OT treatment cessation on body weight, body weight gain, body composition, and energy intake in DIO CD IGS rats. Minipumps were removed on *day 27* (indicated by arrow) from a subset of DIO rats ($n = 6$/group) that had received continuous infusions of vehicle or OT (16 nmol/day). Ad libitum-fed rats were maintained on the HFD (60% of kcal from fat) throughout the 27-day washout period. *A*: change in body weight in HFD-fed DIO animals during washout. *B*: change in body weight gain in HFD-fed DIO animals during washout. *C*: change in fat mass and lean mass in HFD-fed DIO animals during washout. *D*: daily energy intake in HFD-fed DIO animals during washout. Values are means ± SE. $^*P < 0.05$, OT vs. vehicle.

stimulation of BAT thermogenesis in OT-elicited weight loss (Fig. 9).

DISCUSSION

The goal of the current studies was to determine *1*) whether, during chronic infusion, hindbrain (4V) OT recapitulates the ability of 3V OT to elicit sustained weight loss in rodent models of DIO and *2*) whether this effect involves increased IBAT thermogenesis in addition to reduced energy intake. Our findings demonstrate that, in a rat model of DIO, chronic 4V administration of OT effectively recapitulates the antiobesity effect elicited by infusion into the 3V. We also report that that OT injection into the 3V or 4V acutely elevates T_{IBAT}, a functional readout of BAT thermogenesis in vivo, and that these effects are mediated via an OTR-dependent mechanism. Collectively, these findings support the hypothesis that OT action in the hindbrain evokes weight loss in DIO rodents by reducing HFD intake while simultaneously increasing BAT thermogenesis.

Our finding that chronic hindbrain (4V) administration of OT evokes weight loss in DIO HFD-fed rats extends previous evidence from studies in which *1*) 4V OT administered acutely to rats reduced standard chow intake (27, 43), and *2*) chronic OT administration into the lateral ventricle or 3V of rats and mice reduced HFD intake and body weight (7, 17, 59, 60). While activation of OTRs in the arcuate nucleus (34), ventromedial hypothalamus (VMH) (41), or other forebrain areas may contribute to the weight-reducing effects of 3V OT, our finding that 4V administration recapitulates these effects suggests that activation of hindbrain OTRs is sufficient to explain this effect. While it is conceivable that some effects of 4V administration resulted from reflux into the 3V and activation of forebrain OTRs, such an effect could have made only a small contribution to the effects we observed. This assertion is based on previous evidence demonstrating that *1*) angiotensin II, which acts through forebrain type 1 (AT_1) receptors, fails to stimulate drinking behavior following 4V administration (21) and *2*) 4V administration of India ink does not result in ink distribution rostral to the caudal brain stem (22, 25). Nevertheless, future studies to exclude this possibility are warranted, as are studies to determine whether hindbrain OTRs are necessary for the antiobesity effects of OT. Specifically, it will be important to address the extent to which deletion of NTS OTRs in both mice and rats fed a HFD *1*) blocks the effects of chronic 4V OT to reduce HFD intake, increase EE, and induce weight loss and *2*) predisposes animals to DIO and associated metabolic defects.

Our finding that BAT thermogenesis increases following 4V OT administration implicates hindbrain and/or spinal cord OTR populations in these effects. This interpretation is consistent with anatomic evidence indicating that OT neuronal cell bodies in the parvocellular neurons of the PVN are positioned to control sympathetic nervous system (SNS) outflow to IBAT to stimulate BAT thermogenesis through direct descending projections to the hindbrain NTS (47, 50) and/or spinal cord (50), sites that can control SNS outflow to IBAT and are linked to the control of BAT thermogenesis (2, 13). Theoretically, OT action on NTS neurons could influence BAT thermogenesis directly via projections to the spinal cord (whether OTR-expressing premotor NTS neurons project to the spinal cord remains to be determined) or indirectly via projections to sympathetic premotor neurons in the raphe pallidus (RPa) (31). Neurons in the RPa regulate SNS control of BAT via projections to sympathetic preganglionic neurons in the spinal cord in a circuit that is essential for normal thermoregulation (13, 36, 38). Since neurons in this brain area also express OTRs that are activated by cold exposure (30), OT-mediated BAT thermogenesis may also involve activation of OTRs within the RPa. Consistent with this hypothesis is evidence that, in mice that lack OTRs, virally mediated rescue of OTRs, specifically in the rostral RPa, is sufficient to rescue impairments of thermogenesis and IBAT activation by cold exposure (30). Histological analysis revealed that these effects coincided with "scarce" accumulation of lipid droplets in IBAT (30) compared with the excessive number of lipid droplets in IBAT of OTR-null mice (consistent with hypoactivity of BAT and impaired thermogenesis) (54). Future studies are warranted to more clearly delineate the OTR-expressing neuronal population(s) responsible for OT-induced BAT thermogenesis and determine the extent to which the antiobesity effect of OT depends on this mechanism.

The more robust effect of OT in DIO animals may be explained by a number of factors, including macronutrient preference toward fat and/or the presence of cholesterol in the HFD, which may enhance the affinity state of the OTR (3, 24).

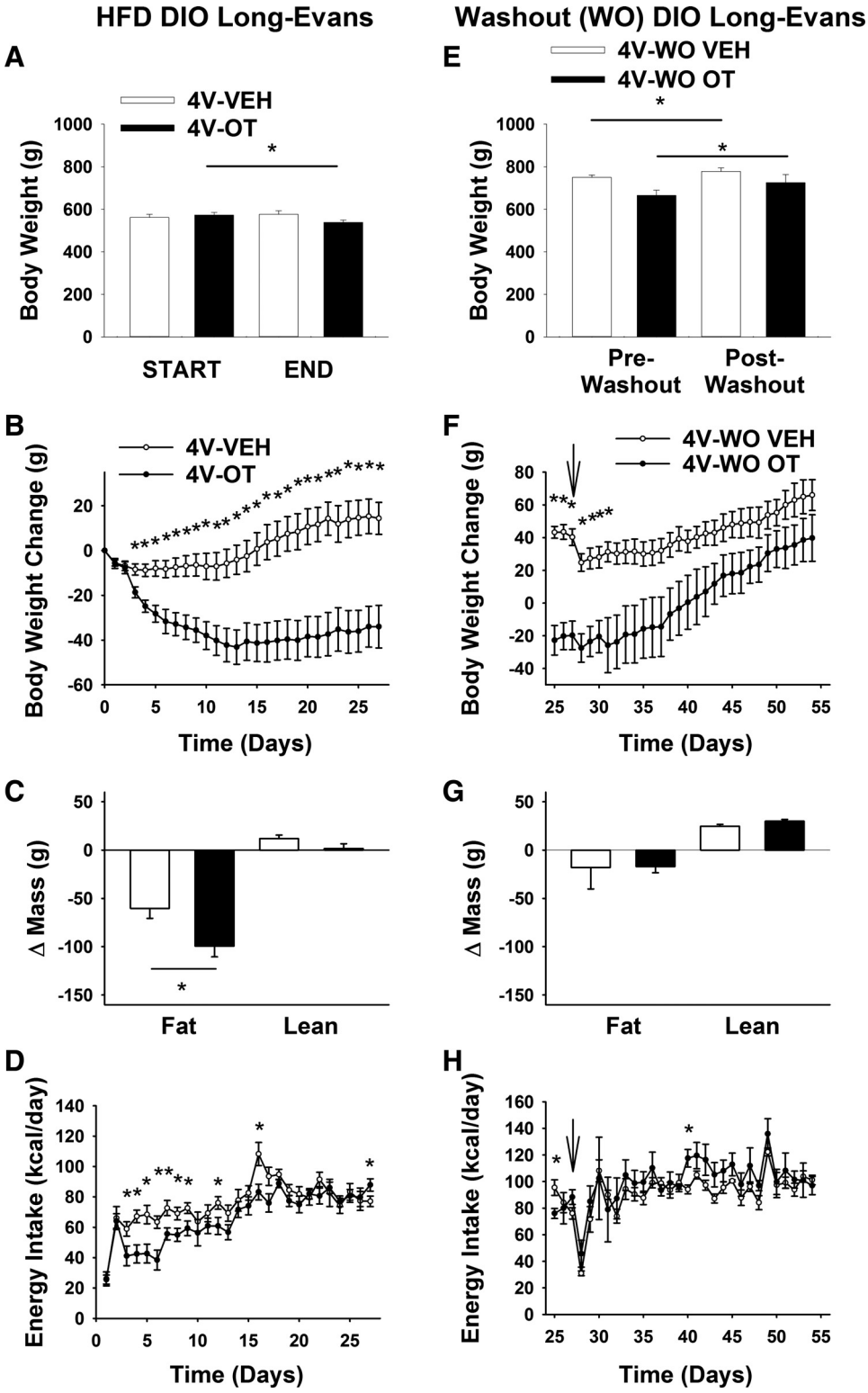

Fig. 6. Effects of chronic 4V OT infusions and 4V OT treatment cessation on energy intake, body weight gain, and body composition in DIO Long-Evans rats. Ad libitum-fed rats were maintained on the HFD (60% of kcal from fat; $n = 6–8$/group) for 4.5 mo before receiving continuous infusions of vehicle or OT (16 nmol/day). Minipumps were removed on *day 27* (indicated by arrow) from a subset of DIO rats ($n = 4$/group), and animals were maintained on the HFD throughout the 27-day washout period. *A* and *E*: change in body weight in HFD-fed DIO animals during treatment and washout. *B* and *F*: change in body weight gain in HFD-fed DIO animals during treatment and washout. *C* and *G*: change in fat mass and lean mass in HFD-fed DIO animals during treatment and washout. *D* and *H*: daily energy intake in HFD-fed DIO animals during treatment and washout. Values are means ± SE. $*P < 0.05$, OT vs. vehicle or post-OT vs. postvehicle.

Our previous work sought to gain insight into whether the ability of OT to induce weight loss is influenced by *1*) diet composition, *2*) adiposity, or *3*) body weight (7), as well as whether 3V OT is sufficient to prevent DIO, induce weight loss in DIO rodents, or both. Our finding that chronic 3V OT preferentially reduces energy intake and prevents weight gain in HFD-fed DIO rat models, even when their body weight and adiposity are comparable to chow-fed controls (7), suggests that the selective nature of the weight-reducing effect of central OT is influenced more by diet composition than by differences in body weight or adiposity. Whether the same is true following 4V OT treatment is a priority for future studies.

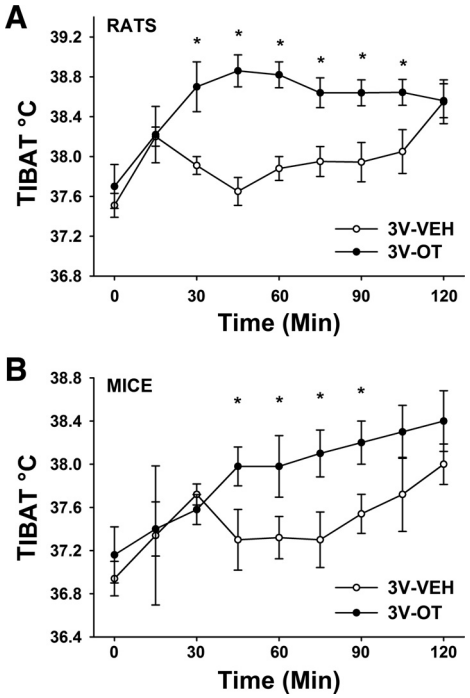

Fig. 7. Effects of 3V OT administration on interscapular brown adipose tissue temperature (T_{IBAT}) in rats and mice. *A*: T_{IBAT} in rats that received acute 3V injections of OT (5 μg/μl) or vehicle (n = 10/group). *B*: T_{IBAT} in mice that received an acute 3V injection of OT (5 μg/μl; n = 5/group). Values are means ± SE. *$P < 0.05$, OT vs. vehicle.

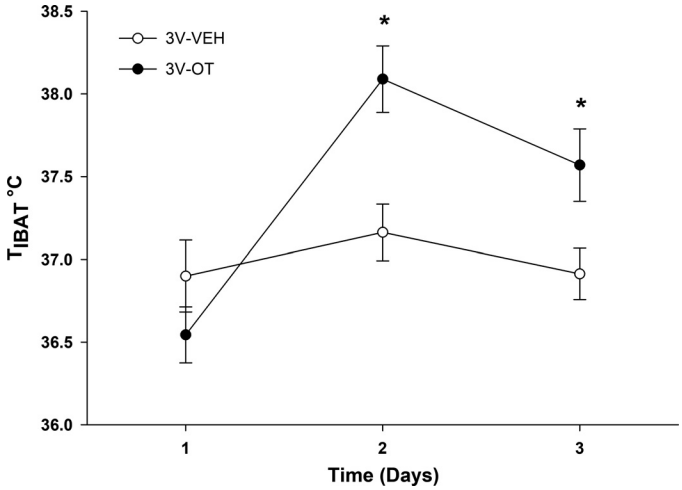

Fig. 9. Effects of chronic 3V OT administration on T_{IBAT} in DIO Long-Evans rats. T_{IBAT} was measured daily during 72-h infusions of OT (16 nmol/day) or vehicle in 3-h-fasted rats (n = 8–10/group). Values are means ± SE. *$P < 0.05$, OT vs. vehicle.

Rosenbaum and colleagues propose that weight loss in obese humans produces a state of relative leptin deficiency that activates orexigenic and energy conservation mechanisms to limit weight loss and promote weight regain (48, 49). In this context, it is noteworthy that *1*) weight loss induced by 4V OT persists for ~4–5 days following cessation of treatment and *2*) animals do not increase their food intake during this time. Thus the action of OT in the hindbrain may maintain weight loss by preventing the rebound hyperphagia that is normally associated with energy deficit. Similar effects were observed following cessation of OT treatment in CD IGS rats (7), DIO mice (33), and nonhuman primates (4). By comparison, rebound hyperphagia occurs within 1–3 days following treatment cessation with melanotan II (44), exendin-4 (46), or an exendin-4/peptide YY-(3–36) cocktail (46). The prolonged carryover effect of OT is not unique to effects on energy balance, however, as the effects of OT on exploratory and antiaggressive behavior also persist for ≥7 days following cessation of treatment in male rats (10). A priority for future work is identification of energy balance neurocircuits on which OT acts to maintain weight loss following treatment cessation.

One caveat to these considerations is that cessation of OT treatment elicited rebound hyperphagia in the Long-Evans DIO rat model, but not in CD IGS rats. These findings are consistent with a recent study that compared mechanisms accounting for rebound weight gain (i.e., rebound hyperphagia with or without reduced EE) in Long-Evans and Sprague-Dawley rats (CD IGS rats are derived from the Sprague-Dawley rat strain; personal communication, Charles River Laboratories) that were allowed to refeed following a prolonged bout of calorie restriction (20). Evans et al. found that Long-Evans rats display an immediate rebound hyperphagia that persists for ~8 days and, in addition,

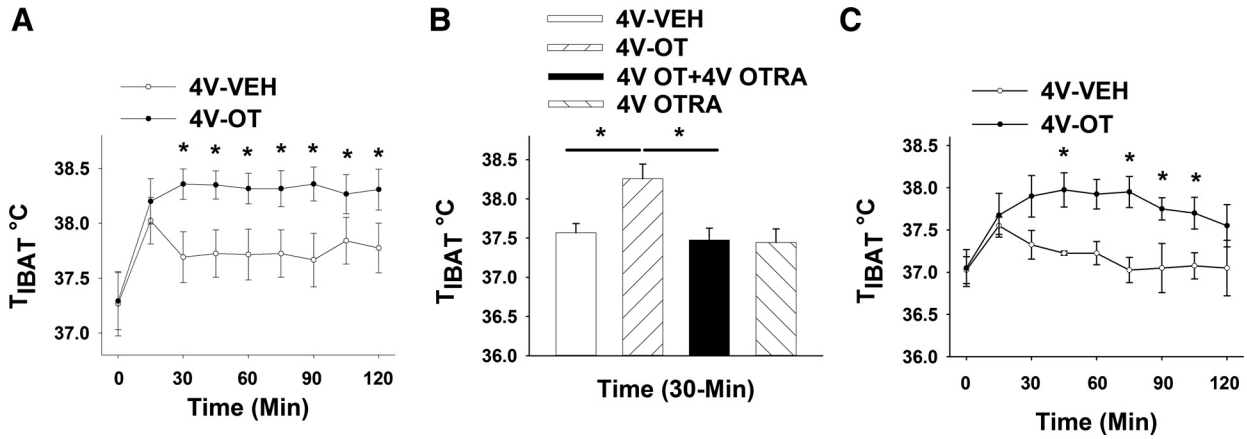

Fig. 8. Effects of 4V OT administration on T_{IBAT} in chow-fed and HFD-fed DIO Long-Evans rats. *A*: T_{IBAT} in rats that received acute 4V injections of OT (5 μg/μl) or vehicle (n = 12/group). *B*: T_{IBAT} in rats that received an acute 4V injection of OT receptor antagonist (OTRA, 10 μg/2 μl) before OT (5 μg/μl; n = 12/group). *C*: T_{IBAT} in DIO rats that received an acute 4V injection (5 μg/μl) or vehicle (n = 4/group). Values are means ± SE. *$P < 0.05$, OT vs. vehicle.

have a more immediate normalization of EE following calorie restriction (20). In contrast, Sprague-Dawley rats show only a mild and transient rebound hyperphagia that was completely resolved by *day 2*. In addition, the Sprague-Dawley rats showed prolonged suppression of EE that persisted for ≥4 days into the refeeding period. These observations are consistent with our finding that, following cessation of OT treatment (and prolonged weight loss), the Long-Evans DIO rat model, but not CD IGS rats, showed a rebound hyperphagia. These findings suggest that mechanisms underlying recovery of lost weight following OT treatment vary with genetic background strain. Future studies that delineate energy balance neurocircuits on which OT acts to elicit its effects on energy homeostasis may shed light on these strain differences.

Perspectives and Significance

Obesity and its associated metabolic complications (15, 19, 26) are major health concerns (51). According to the World Health Organization, global obesity prevalence rates have increased at least twofold since 1980, with ~1.9 billion adults classified as being overweight as of 2014 (Fact Sheet No. 311, World Health Organization). In the United States alone, obesity impacts ~78 million adults and 12.5 million children and adolescents (42). Given the limited efficacy of current treatment options, the need for new, more effective approaches is urgent.

Our current work documents combined effects of OT action in the hindbrain to reduce energy intake and increase BAT thermogenesis, with the result that body fat content is reduced in a manner that is sustained through several weeks of treatment. Moreover, OT-induced weight loss cannot be attributed to an aversive effect, is not observed in nonobese rats fed standard chow, and spares lean mass. Each of these features is highly desirable for an obesity therapeutic agent, especially given that, in humans and nonhuman primates, OT can be administered intranasally (14, 32, 61). This delivery method holds promise as an appealing, noninvasive strategy to target OTRs in the CNS that regulate appetite and/or BAT thermogenesis (23, 53).

Since previous effects of intranasal OT on energy balance have focused primarily on food intake, further studies are warranted to identify the extent to which intranasal OT increases BAT thermogenesis and EE in rodent and nonhuman primate models and the extent to which hindbrain OTRs mediate these effects. Intranasal OT may also be effective for prevention of weight gain among those at risk, including patients taking certain antipsychotic medications (52). For example, the effect of the antipsychotic olanzapine to cause marked weight gain involves increased intake and reduced EE and BAT thermogenesis (52). Thus intranasal OT could potentially be used as an adjunct to prevent the weight gain associated with these drugs. Future studies that address the extent to which chronic intranasal OT can safely and effectively reverse or prevent obesity in humans are a priority.

ACKNOWLEDGMENTS

The authors acknowledge the technical support of Lindsey Masewicz, Shari Wang, and Brian Van Yserloo. The authors particularly acknowledge the assistance of Dr. Timothy Bartness (deceased), who was instrumental in providing input on several aspects of experimental design and specific methodologies required for T_{IBAT} measurements. The authors are grateful to Drs. Denis Baskin and Gerald Taborsky, Jr., for feedback throughout the course of these studies.

GRANTS

This material was based on work supported by the Office of Research and Development, Medical Research Service, Department of Veterans Affairs (VA) and the VA Puget Sound Health Care System Rodent Metabolic and Behavioral Phenotyping Core. This work was supported by US Department of Veterans Affairs Biomedical Laboratory Research and Development Service Merit Review Award 5I01BX001213-04; the University of Washington Nutrition Obesity Research Center Adipose Tissue and Obesity Core, with support from National Institutes of Health (NIH) Grant P30 DK-035816; and the University of Washington Diabetes Research Center Vector and Transgenic Mouse Core and the University of Washington Diabetes Research Center Cellular and Molecular Imaging Core, with support from NIH Grant P30 DK-017047. P. J. Havel's research program is also supported by NIH Grants DK-095980, HL-091333, HL-107256, and HL-107256 and a Multi-Campus Grant from the University of California Office of the President.

DISCLAIMERS

The contents do not represent the views of the US Department of Veterans Affairs or the US Government.

DISCLOSURES

J. E. Blevins is a consultant for OXT Therapeutics, Inc. and has stock options.

AUTHOR CONTRIBUTIONS

M.E.M., V.R., C.H.V., M.W.S. G.J.M. and J.E.B conceived and designed research; Z.S.R., T.H.W.-H., J.L.G., D.W.C., and J.E.B. performed experiments; Z.S.R., T.H.W.-H., M.E.M., V.R., C.H.V., J.L.G., P.J.H., M.W.S., G.J.M., and J.E.B. edited and revised manuscript; Z.S.R., T.H.W.-H., M.E.M., V.R., C.H.V., J.L.G., P.J.H., M.W.S., G.J.M., and J.E.B. approved final version of manuscript; J.L.G. and J.E.B. analyzed data; J.L.G., P.J.H., M.W.S., G.J.M., and J.E.B. interpreted results of experiments; J.E.B. prepared figures; J.E.B. drafted manuscript.

REFERENCES

1. **Altirriba J, Poher AL, Caillon A, Arsenijevic D, Veyrat-Durebex C, Lyautey J, Dulloo A, Rohner-Jeanrenaud F.** Divergent effects of oxytocin treatment of obese diabetic mice on adiposity and diabetes. *Endocrinology* 155: 4189–4201, 2014. doi:10.1210/en.2014-1466.
2. **Bamshad M, Song CK, Bartness TJ.** CNS origins of the sympathetic nervous system outflow to brown adipose tissue. *Am J Physiol Regul Integr Comp Physiol* 276: R1569–R1578, 1999.
3. **Blevins JE, Baskin DG.** Translational and therapeutic potential of oxytocin as an anti-obesity strategy: insights from rodents, nonhuman primates and humans. *Physiol Behav* 152: 438–449, 2015. doi:10.1016/j.physbeh.2015.05.023.
4. **Blevins JE, Graham JL, Morton GJ, Bales KL, Schwartz MW, Baskin DG, Havel PJ.** Chronic oxytocin administration inhibits food intake, increases energy expenditure, and produces weight loss in fructose-fed obese rhesus monkeys. *Am J Physiol Regul Integr Comp Physiol* 308: R431–R438, 2015. doi:10.1152/ajpregu.00441.2014.
6. **Blevins JE, Schwartz MW, Baskin DG.** Evidence that paraventricular nucleus oxytocin neurons link hypothalamic leptin action to caudal brain stem nuclei controlling meal size. *Am J Physiol Regul Integr Comp Physiol* 287: R87–R96, 2004. doi:10.1152/ajpregu.00604.2003.
7. **Blevins JE, Thompson BW, Anekonda VT, Ho JM, Graham JL, Roberts ZS, Hwang BH, Ogimoto K, Wolden-Hanson TH, Nelson JO, Kaiyala KJ, Havel PJ, Bales KL, Morton GJ, Schwartz MW, Baskin DG.** Chronic CNS oxytocin signaling preferentially induces fat loss in high fat diet-fed rats by enhancing satiety responses and increasing lipid utilization. *Am J Physiol Regul Integr Comp Physiol* 310: R640–658 2016. doi:10.1152/ajpregu.00220.2015.
8. **Bremer AA, Stanhope KL, Graham JL, Cummings BP, Wang W, Saville BR, Havel PJ.** Fructose-fed rhesus monkeys: a nonhuman primate model of insulin resistance, metabolic syndrome, and type 2 diabetes. *Clin Transl Sci* 4: 243–252, 2011. doi:10.1111/j.1752-8062.2011.00298.x.
9. **Brito MN, Brito NA, Baro DJ, Song CK, Bartness TJ.** Differential activation of the sympathetic innervation of adipose tissues by melano-

cortin receptor stimulation. *Endocrinology* 148: 5339–5347, 2007. doi:10.1210/en.2007-0621.

10. **Calcagnoli F, Meyer N, de Boer SF, Althaus M, Koolhaas JM.** Chronic enhancement of brain oxytocin levels causes enduring anti-aggressive and pro-social explorative behavioral effects in male rats. *Horm Behav* 65: 427–433, 2014. doi:10.1016/j.yhbeh.2014.03.008.
11. **Camerino C.** Low sympathetic tone and obese phenotype in oxytocin-deficient mice. *Obesity (Silver Spring)* 17: 980–984, 2009. doi:10.1038/oby.2009.12.
12. **Cannon B, Nedergaard J.** Brown adipose tissue: function and physiological significance. *Physiol Rev* 84: 277–359, 2004. doi:10.1152/physrev.00015.2003.
13. **Cano G, Passerin AM, Schiltz JC, Card JP, Morrison SF, Sved AF.** Anatomical substrates for the central control of sympathetic outflow to interscapular adipose tissue during cold exposure. *J Comp Neurol* 460: 303–326, 2003. doi:10.1002/cne.10643.
14. **Chang SW, Platt ML.** Oxytocin and social cognition in rhesus macaques: implications for understanding and treating human psychopathology. *Brain Res* 1580: 57–68, 2014. doi:10.1016/j.brainres.2013.11.006.
15. **Cornier MA, Dabelea D, Hernandez TL, Lindstrom RC, Steig AJ, Stob NR, Van Pelt RE, Wang H, Eckel RH.** The metabolic syndrome. *Endocr Rev* 29: 777–822, 2008. doi:10.1210/er.2008-0024.
16. **Cummings BP, Digitale EK, Stanhope KL, Graham JL, Baskin DG, Reed BJ, Sweet IR, Griffen SC, Havel PJ.** Development and characterization of a novel rat model of type 2 diabetes mellitus: the UC Davis type 2 diabetes mellitus UCD-T2DM rat. *Am J Physiol Regul Integr Comp Physiol* 295: R1782–R1793, 2008. doi:10.1152/ajpregu.90635.2008.
17. **Deblon N, Veyrat-Durebex C, Bourgoin L, Caillon A, Bussier AL, Petrosino S, Piscitelli F, Legros JJ, Geenen V, Foti M, Wahli W, Di Marzo V, Rohner-Jeanrenaud F.** Mechanisms of the anti-obesity effects of oxytocin in diet-induced obese rats. *PLoS One* 6: e25565, 2011. doi:10.1371/journal.pone.0025565.
18. **Dorfman MD, Krull JE, Douglass JD, Fasnacht R, Lara-Lince F, Meek TH, Shi X, Damian V, Nguyen HT, Matsen ME, Morton GJ, Thaler JP.** Sex differences in microglial CX3CR1 signalling determine obesity susceptibility in mice. *Nat Commun* 8: 14556, 2017. doi:10.1038/ncomms14556.
19. **Eckel RH, Grundy SM, Zimmet PZ.** The metabolic syndrome. *Lancet* 365: 1415–1428, 2005. doi:10.1016/S0140-6736(05)66378-7.
20. **Evans SA, Messina MM, Knight WD, Parsons AD, Overton JM.** Long-Evans and Sprague-Dawley rats exhibit divergent responses to refeeding after caloric restriction. *Am J Physiol Regul Integr Comp Physiol* 288: R1468–R1476, 2005. doi:10.1152/ajpregu.00602.2004.
21. **Fitzsimons JT, Kucharczyk J.** Drinking and haemodynamic changes induced in the dog by intracranial injection of components of the renin-angiotensin system. *J Physiol* 276: 419–434, 1978. doi:10.1113/jphysiol.1978.sp012244.
22. **Flynn FW, Grill HJ.** Fourth ventricular phlorizin dissociates feeding from hyperglycemia in rats. *Brain Res* 341: 331–336, 1985. doi:10.1016/0006-8993(85)91072-8.
23. **Freeman SM, Samineni S, Allen PC, Stockinger D, Bales KL, Hwa GG, Roberts JA.** Plasma and CSF oxytocin levels after intranasal and intravenous oxytocin in awake macaques. *Psychoneuroendocrinology* 66: 185–194, 2016. doi:10.1016/j.psyneuen.2016.01.014.
24. **Gimpl G, Fahrenholz F.** The oxytocin receptor system: structure, function, and regulation. *Physiol Rev* 81: 629–683, 2001.
25. **Grill HJ, Donahey JC, King L, Kaplan JM.** Contribution of caudal brainstem to *d*-fenfluramine anorexia. *Psychopharmacology (Berl)* 130: 375–381, 1997. doi:10.1007/s002130050253.
26. **Grundy SM.** Metabolic syndrome pandemic. *Arterioscler Thromb Vasc Biol* 28: 629–636, 2008. doi:10.1161/ATVBAHA.107.151092.
27. **Ho JM, Anekonda VT, Thompson BW, Zhu M, Curry RW, Hwang BH, Morton GJ, Schwartz MW, Baskin DG, Appleyard SM, Blevins JE.** Hindbrain oxytocin receptors contribute to the effects of circulating oxytocin on food intake in male rats. *Endocrinology* 155: 2845–2857, 2014. doi:10.1210/en.2014-1148.
28. **Iwasaki Y, Maejima Y, Suyama S, Yoshida M, Arai T, Katsurada K, Kumari P, Nakabayashi H, Kakei M, Yada T.** Peripheral oxytocin activates vagal afferent neurons to suppress feeding in normal and leptin-resistant mice: a route for ameliorating hyperphagia and obesity. *Am J Physiol Regul Integr Comp Physiol* 308: R360–R369, 2015. doi:10.1152/ajpregu.00344.2014.
29. **Kasahara Y, Sato K, Takayanagi Y, Mizukami H, Ozawa K, Hidema S, So KH, Kawada T, Inoue N, Ikeda I, Roh SG, Itoi K, Nishimori K.** Oxytocin receptor in the hypothalamus is sufficient to rescue normal thermoregulatory function in male oxytocin receptor knockout mice. *Endocrinology* 154: 4305–4315, 2013. doi:10.1210/en.2012-2206.
30. **Kasahara Y, Tateishi Y, Hiraoka Y, Otsuka A, Mizukami H, Ozawa K, Sato K, Hidema S, Nishimori K.** Role of the oxytocin receptor expressed in the rostral medullary raphe in thermoregulation during cold conditions. *Front Endocrinol (Lausanne)* 6: 180, 2015.
31. **Kong D, Tong Q, Ye C, Koda S, Fuller PM, Krashes MJ, Vong L, Ray RS, Olson DP, Lowell BB.** GABAergic RIP-Cre neurons in the arcuate nucleus selectively regulate energy expenditure. *Cell* 151: 645–657, 2012. doi:10.1016/j.cell.2012.09.020.
32. **Lawson EA, Marengi DA, DeSanti RL, Holmes TM, Schoenfeld DA, Tolley CJ.** Oxytocin reduces caloric intake in men. *Obesity (Silver Spring)* 23: 950–956, 2015. doi:10.1002/oby.21069.
33. **Maejima Y, Iwasaki Y, Yamahara Y, Kodaira M, Sedbazar U, Yada T.** Peripheral oxytocin treatment ameliorates obesity by reducing food intake and visceral fat mass. *Aging (Albany NY)* 3: 1169–1177, 2011. doi:10.18632/aging.100408.
34. **Maejima Y, Sakuma K, Santoso P, Gantulga D, Katsurada K, Ueta Y, Hiraoka Y, Nishimori K, Tanaka S, Shimomura K, Yada T.** Oxytocinergic circuit from paraventricular and supraoptic nuclei to arcuate POMC neurons in hypothalamus. *FEBS Lett* 588: 4404–4412, 2014. doi:10.1016/j.febslet.2014.10.010.
35. **Maejima Y, Sedbazar U, Suyama S, Kohno D, Onaka T, Takano E, Yoshida N, Koike M, Uchiyama Y, Fujiwara K, Yashiro T, Horvath TL, Dietrich MO, Tanaka S, Dezaki K, Oh-I S, Hashimoto K, Shimizu H, Nakata M, Mori M, Yada T.** Nesfatin-1-regulated oxytocinergic signaling in the paraventricular nucleus causes anorexia through a leptin-independent melanocortin pathway. *Cell Metab* 10: 355–365, 2009. doi:10.1016/j.cmet.2009.09.002.
36. **Morrison SF.** Central control of body temperature. *F1000 Res* 5: 880, 2016. doi:10.12688/f1000research.7958.1.
37. **Morrison SF, Madden CJ, Tupone D.** Central neural regulation of brown adipose tissue thermogenesis and energy expenditure. *Cell Metab* 19: 741–756, 2014. doi:10.1016/j.cmet.2014.02.007.
39. **Morton GJ, Matsen ME, Bracy DP, Meek TH, Nguyen HT, Stefanovski D, Bergman RN, Wasserman DH, Schwartz MW.** FGF19 action in the brain induces insulin-independent glucose lowering. *J Clin Invest* 123: 4799–4808, 2013. doi:10.1172/JCI70710.
40. **Morton GJ, Thatcher BS, Reidelberger RD, Ogimoto K, Wolden-Hanson T, Baskin DG, Schwartz MW, Blevins JE.** Peripheral oxytocin suppresses food intake and causes weight loss in diet-induced obese rats. *Am J Physiol Endocrinol Metab* 302: E134–E144, 2012. doi:10.1152/ajpendo.00296.2011.
41. **Noble EE, Billington CJ, Kotz CM, Wang C.** Oxytocin in the ventromedial hypothalamic nucleus reduces feeding and acutely increases energy expenditure. *Am J Physiol Regul Integr Comp Physiol* 307: R737–R745, 2014. doi:10.1152/ajpregu.00118.2014.
42. **Ogden CL, Carroll MD, Kit BK, Flegal KM.** Prevalence of obesity in the United States, 2009–2010. *NCHS Data Brief* 82: 1–8, 2012.
43. **Ong ZY, Alhadeff AL, Grill HJ.** Medial nucleus tractus solitarius oxytocin receptor signaling and food intake control: the role of gastrointestinal satiation signal processing. *Am J Physiol Regul Integr Comp Physiol* 308: R800–R806, 2015. doi:10.1152/ajpregu.00534.2014.
44. **Pierroz DD, Ziotopoulou M, Ungsunan L, Moschos S, Flier JS, Mantzoros CS.** Effects of acute and chronic administration of the melanocortin agonist MTII in mice with diet-induced obesity. *Diabetes* 51: 1337–1345, 2002. doi:10.2337/diabetes.51.5.1337.
45. **Plante E, Menaouar A, Danalache BA, Yip D, Broderick TL, Chiasson JL, Jankowski M, Gutkowska J.** Oxytocin treatment prevents the cardiomyopathy observed in obese diabetic male *db/db* mice. *Endocrinology* 156: 1416–1428, 2015. doi:10.1210/en.2014-1718.
46. **Reidelberger RD, Haver AC, Apenteng BA, Anders KL, Steenson SM.** Effects of exendin-4 alone and with peptide YY(3-36) on food intake and body weight in diet-induced obese rats. *Obesity (Silver Spring)* 19: 121–127, 2011. doi:10.1038/oby.2010.136.
47. **Rinaman L.** Oxytocinergic inputs to the nucleus of the solitary tract and dorsal motor nucleus of the vagus in neonatal rats. *J Comp Neurol* 399: 101–109, 1998. doi:10.1002/(SICI)1096-9861(19980914)399:1<101::AID-CNE8>3.0.CO;2-5.
48. **Rosenbaum M, Kissileff HR, Mayer LE, Hirsch J, Leibel RL.** Energy intake in weight-reduced humans. *Brain Res* 1350: 95–102, 2010. doi:10.1016/j.brainres.2010.05.062.

49. **Rosenbaum M, Leibel RL.** Adaptive thermogenesis in humans. *Int J Obes* 34, *Suppl* 1: S47–S55, 2010. doi:10.1038/ijo.2010.184.
50. **Sawchenko PE, Swanson LW.** Immunohistochemical identification of neurons in the paraventricular nucleus of the hypothalamus that project to the medulla or to the spinal cord in the rat. *J Comp Neurol* 205: 260–272, 1982. doi:10.1002/cne.902050306.
51. **Smyth S, Heron A.** Diabetes and obesity: the twin epidemics. *Nat Med* 12: 75–80, 2006. doi:10.1038/nm0106-75.
52. **Stefanidis A, Verty AN, Allen AM, Owens NC, Cowley MA, Oldfield BJ.** The role of thermogenesis in antipsychotic drug-induced weight gain. *Obesity (Silver Spring)* 17: 16–24, 2009. doi:10.1038/oby.2008.468.
53. **Striepens N, Kendrick KM, Hanking V, Landgraf R, Wüllner U, Maier W, Hurlemann R.** Elevated cerebrospinal fluid and blood concentrations of oxytocin following its intranasal administration in humans. *Sci Rep* 3: 3440, 2013. doi:10.1038/srep03440.

53a. **Sutton AK, Pei H, Burnett KH, Myers MG Jr, Rhodes CJ, Olson DP.** Control of food intake and energy expenditure by Nos1 neurons of the paraventricular hypothalamus. *J Neurosci* 12: 15306–15318, 2014. doi:10.1523/JNEUROSCI.0226-14.2014.

54. **Takayanagi Y, Kasahara Y, Onaka T, Takahashi N, Kawada T, Nishimori K.** Oxytocin receptor-deficient mice developed late-onset obesity. *Neuroreport* 19: 951–955, 2008. doi:10.1097/WNR.0b013e3283021ca9.
55. **Thaler JP, Yi CX, Schur EA, Guyenet SJ, Hwang BH, Dietrich MO, Zhao X, Sarruf DA, Izgur V, Maravilla KR, Nguyen HT, Fischer JD, Matsen ME, Wisse BE, Morton GJ, Horvath TL, Baskin DG, Tschöp MH, Schwartz MW.** Obesity is associated with hypothalamic injury in rodents and humans. *J Clin Invest* 122: 153–162, 2012. doi:10.1172/JCI59660.
56. **Thienel M, Fritsche A, Heinrichs M, Peter A, Ewers M, Lehnert H, Born J, Hallschmid M.** Oxytocin's inhibitory effect on food intake is stronger in obese than normal-weight men. *Int J Obes* 40: 1707–1714, 2016. doi:10.1038/ijo.2016.149.
57. **Vaughan CH, Shrestha YB, Bartness TJ.** Characterization of a novel melanocortin receptor-containing node in the SNS outflow circuitry to brown adipose tissue involved in thermogenesis. *Brain Res* 1411: 17–27, 2011. doi:10.1016/j.brainres.2011.07.003.
58. **Wu Z, Xu Y, Zhu Y, Sutton AK, Zhao R, Lowell BB, Olson DP, Tong Q.** An obligate role of oxytocin neurons in diet induced energy expenditure. *PLoS One* 7: e45167, 2012. doi:10.1371/journal.pone.0045167.
59. **Zhang G, Bai H, Zhang H, Dean C, Wu Q, Li J, Guariglia S, Meng Q, Cai D.** Neuropeptide exocytosis involving synaptotagmin-4 and oxytocin in hypothalamic programming of body weight and energy balance. *Neuron* 69: 523–535, 2011. doi:10.1016/j.neuron.2010.12.036.
60. **Zhang G, Cai D.** Circadian intervention of obesity development via resting-stage feeding manipulation or oxytocin treatment. *Am J Physiol Endocrinol Metab* 301: E1004–E1012, 2011. doi:10.1152/ajpendo.00196.2011.
61. **Zhang H, Wu C, Chen Q, Chen X, Xu Z, Wu J, Cai D.** Treatment of obesity and diabetes using oxytocin or analogs in patients and mouse models. *PLoS One* 8: e61477, 2013. doi:10.1371/journal.pone.0061477.